



University of Warwick institutional repository: <http://go.warwick.ac.uk/wrap>

This paper is made available online in accordance with publisher policies. Please scroll down to view the document itself. Please refer to the repository record for this item and our policy information available from the repository home page for further information.

To see the final version of this paper please visit the publisher's website. Access to the published version may require a subscription.

Author(s): Robert T. R. Huckstepp and Nicholas Dale

Article Title: CO<sub>2</sub>-dependent opening of an inwardly rectifying K<sup>+</sup> channel

Year of publication: 2011

Link to published article:

<http://dx.doi.org/10.1007/s00424-010-0916-z>

Publisher statement: None

# CO<sub>2</sub>-dependent opening of an inwardly rectifying K<sup>+</sup> channel

Robert T. R. Huckstepp · Nicholas Dale

Received: 9 November 2010 / Revised: 11 December 2010 / Accepted: 17 December 2010 / Published online: 14 January 2011  
© The Author(s) 2011. This article is published with open access at Springerlink.com

**Abstract** CO<sub>2</sub> chemosensing is a vital function for the maintenance of life that helps to control acid–base balance. Most studies have reported that CO<sub>2</sub> is measured via its proxy, pH. Here we report an inwardly rectifying channel, in outside-out excised patches from HeLa cells that was sensitive to modest changes in PCO<sub>2</sub> under conditions of constant extracellular pH. As PCO<sub>2</sub> increased, the open probability of the channel increased. The single-channel currents had a conductance of 6.7 pS and a reversal potential of –70 mV, which lay between the K<sup>+</sup> and Cl<sup>–</sup> equilibrium potentials. This reversal potential was shifted by +61 mV following a tenfold increase in extracellular [K<sup>+</sup>] but was insensitive to variations of extracellular [Cl<sup>–</sup>]. The single-channel conductance increased with extracellular [K<sup>+</sup>]. We propose that this channel is a member of the Kir family. In addition to this K<sup>+</sup> channel, we found that many of the excised patches also contained a conductance carried via a Cl<sup>–</sup>-selective channel. This CO<sub>2</sub>-sensitive Kir channel may hyperpolarize excitable cells and provides a potential mechanism for CO<sub>2</sub>-dependent inhibition during hypercapnia.

**Keywords** CO<sub>2</sub> · Kir · Inward rectifier · Chemosensitivity · Transducer · Hyperpolarization · Secretion

## Introduction

Regulation of the levels of blood gases (oxygen and carbon dioxide) is vitally important in the maintenance of life. Of

the two gases, CO<sub>2</sub> appears to be the more powerful stimulant, as PCO<sub>2</sub> in arterial blood is very well controlled at a range of increasing altitudes even though atmospheric PO<sub>2</sub> decreases [8]. Only when extreme altitudes (3,800–4,300 m) are reached or a prolonged period is spent at altitude [2] does the regulation of arterial PCO<sub>2</sub> change. By contrast arterial PO<sub>2</sub> varies dramatically during short-term exposure to moderate altitude; therefore, arterial PCO<sub>2</sub> is tightly regulated at the expense of PO<sub>2</sub> [8].

CO<sub>2</sub> combines with water to form H<sub>2</sub>CO<sub>3</sub>. This reaction is slow and its rate can be dramatically increased by carbonic anhydrase. Once formed H<sub>2</sub>CO<sub>3</sub> rapidly dissociates to HCO<sub>3</sub><sup>–</sup> and H<sup>+</sup>. Thus the level of dissolved CO<sub>2</sub> in the extracellular fluid (ECF) determines its pH. In principle, PCO<sub>2</sub> could be measured in three ways: via CO<sub>2</sub> itself, via pH, or via HCO<sub>3</sub><sup>–</sup>. There is considerable evidence that changes in pH are important in chemoreception; however, evidences for the involvement of HCO<sub>3</sub><sup>–</sup> [22] and CO<sub>2</sub> are beginning to emerge [11, 12]. Although CO<sub>2</sub>/pH-sensitive cells are located in the carotid bodies [18], the major sites of CO<sub>2</sub> chemoreception are found within the brain [4].

To be classified as a primary CO<sub>2</sub>/pH chemosensor, a cell must have certain properties. Firstly, they need to possess a transducer molecule that responds to alterations of CO<sub>2</sub>, HCO<sub>3</sub><sup>–</sup> or pH. Secondly, they have to project to areas responsible for initiating chemoreflexes and finally, once stimulated they must initiate a physiological response [7, 20, 21]. K<sup>+</sup> channels that are highly sensitive to acidification and react by closing are popular candidates for chemosensory transducers. These include the following: TASK (tandem-pore acid sensing potassium channels) 1 and 3 channels [17]; inwardly rectifying potassium channels [19], especially Kir4.1/5.1, and calcium-dependent potassium channels [5]. However, definitive causal evidence linking these channels to behavioral/physiological

R. T. R. Huckstepp · N. Dale (✉)  
School of Life Sciences, University of Warwick,  
Coventry CV4 7AL, UK  
e-mail: N.E.Dale@warwick.ac.uk

responses to changes in  $\text{PCO}_2$  has not yet been achieved. Acid-sensitive cation channels (ASICs) also play a role in at least some  $\text{CO}_2$ -dependent processes [34].

By contrast, there are very few examples of, or putative mechanisms for, direct sensing of  $\text{CO}_2$  [11, 12, 35]. Here we describe a  $\text{K}^+$  channel in HeLa cells that appears to open in a  $\text{CO}_2$ -sensitive manner. If present in neurons this channel would mediate  $\text{CO}_2$ -dependent hyperpolarization and decreased neuronal firing. Though less attention has been paid to inhibitory processes triggered by increases in  $\text{PCO}_2$ , neurons that are inhibited by  $\text{CO}_2$  may be as important as those excited by it [20]. Alternatively, in peripheral tissue this could lead to increased secretion from acinar cells of the major glands.

## Methods

### Cell culture

HeLa cells (either wild type or Cx26 expressing) were maintained in Dulbecco's modified Eagle's medium (DMEM) with the following supplements: 1 mM glutamine (Melford Labs, Suffolk, UK), 10% foetal calf serum (Invitrogen, PaisleyUK), and penicillin/streptomycin (Sigma, St. Louis, MO, USA) at 10 U/ml and 10  $\mu\text{g}$  respectively. In addition, the Cx26 cells were under selective pressure with puromycin (Sigma) at 1  $\mu\text{g}/\text{ml}$ . All cells were grown at 37°C in a humidified 95%  $\text{O}_2/5\%$   $\text{CO}_2$  incubator. For patch clamp recordings, the cells were plated out on glass coverslips in six-well plates at  $2 \times 10^6$  cells/well and used within 3 days from plating.

### Patch clamp recordings

Coverslips containing non-confluent cells were placed into a perfusion chamber at 28°C in sterile filtered control artificial cerebrospinal fluid (aCSF): Standard patch clamp techniques were used to pull outside-out isolated membrane patches. Whole cell patch pipettes were pulled on a Flaming–Brown horizontal puller, Sylgard coated, fire polished, and filled with an intracellular solution: K-gluconate 120 mM,  $\text{CsCl}_2$  10 mM, TEACl 10 mM, EGTA 10 mM, ATP 3 mM,  $\text{MgCl}_2$  1 mM,  $\text{CaCl}_2$  1 mM, sterile filtered, pH adjusted to 7.2 with KOH. After briefly attaining a whole cell recording, isolated patches of the outside-out configuration were excised. To examine the effect of  $\text{PCO}_2$  on channel gating, patches were routinely held at +10 mV. The properties of the  $\text{CO}_2$ -sensitive single-channel current were assessed by taking the patch through a series of 10 mV steps from either +20 or +50 mV to –70 mV in aCSF with a  $\text{PCO}_2$  of 70 mmHg.

An Axopatch 200B amplifier was used (usually in capacitive feedback mode) to record from the membrane patches. The data were low-pass filtered by the amplifier with a cut-off of 2 kHz. The data were sampled by a DT3010 A/D board at 20 kHz. Proprietary software was used to control the experiments and perform offline analysis. For analysis and measurements, the current records were filtered with a Gaussian filter at 0.5 or 0.8 kHz. The reset transients from the feedback capacitor were excluded from analysis (by choosing portions of current records between these transients) and removed from the illustrations in the paper.

### Recording solutions

*Control aCSF* 124 mM NaCl, 3 mM KCl, 1 mM  $\text{CaCl}_2$ , 26 mM  $\text{NaHCO}_3$ , 1.25 mM  $\text{NaH}_2\text{PO}_4$ , 1 mM  $\text{MgSO}_4$ , 10 mM D-glucose saturated with 95%  $\text{O}_2/5\%$   $\text{CO}_2$ , pH 7.5,  $\text{PCO}_2$  35 mmHg.

*$\text{PCO}_2$  70 mmHg aCSF* 70 mM NaCl, 3 mM KCl, 1 mM  $\text{CaCl}_2$ , 80 mM  $\text{NaHCO}_3$ , 1.25 mM  $\text{NaH}_2\text{PO}_4$ , 1 mM  $\text{MgSO}_4$ , 10 mM D-glucose, saturated with approximately 12%  $\text{CO}_2$  (with the balance being  $\text{O}_2$ ) to give a pH of 7.5 and a  $\text{PCO}_2$  of 70 mmHg.

*$\text{PCO}_2$  55 mmHg aCSF* 100 mM NaCl, 3 mM KCl, 1 mM  $\text{CaCl}_2$ , 50 mM  $\text{NaHCO}_3$ , 1.25 mM  $\text{NaH}_2\text{PO}_4$ , 1 mM  $\text{MgSO}_4$ , 10 mM D-glucose, saturated with approximately 9%  $\text{CO}_2$  (with the balance being  $\text{O}_2$ ) to give a pH of 7.5 and a  $\text{PCO}_2$  of 55 mmHg respectively.

*$\text{PCO}_2$  20 mmHg aCSF* 140 mM NaCl, 3 mM KCl, 1 mM  $\text{CaCl}_2$ , 10 mM  $\text{NaHCO}_3$ , 1.25 mM  $\text{NaH}_2\text{PO}_4$ , 1 mM  $\text{MgSO}_4$ , 10 mM D-glucose, saturated with approximately 2%  $\text{CO}_2$  (with the balance being  $\text{O}_2$ ) to give a pH of 7.5 and a  $\text{PCO}_2$  of 20 mmHg.

The level of  $\text{PCO}_2$  was adjusted (by varying the proportion of  $\text{CO}_2$  in the bubbling mixture) so that all solutions had a pH of 7.5. The level of  $\text{PCO}_2$  in these solutions was determined by measurement with a blood gas analyzer [12].

### Ion substitution experiments

To test the nature of the permeant ion, we substituted either  $\text{Cl}^-$  or  $\text{K}^+$ . For  $\text{Cl}^-$  substitution, we used a modified aCSF with Na-gluconate: 10 mM NaCl, 114 mM Na-gluconate, 26 mM  $\text{NaHCO}_3$ , 1.25 mM  $\text{NaH}_2\text{PO}_4$ , 3 mM KCl, 1 mM  $\text{MgSO}_4$ , 1 mM  $\text{CaCl}_2$ , and 10 mM D-glucose, equilibrated with 5%  $\text{CO}_2/95\%$   $\text{O}_2$ .

The patches were also exposed to an isohydric hypercapnic stimulus under conditions of lowered  $\text{Cl}^-$  concen-

trations: 10 mM NaCl, 70 mM Na-gluconate, 80 mM NaHCO<sub>3</sub>, 1.25 mM NaH<sub>2</sub>PO<sub>4</sub>, 3 mM KCl, 1 mM MgSO<sub>4</sub>, 1 mM CaCl<sub>2</sub>, and 10 mM D-glucose, equilibrated with 12% CO<sub>2</sub>/88% O<sub>2</sub>.

To change K<sup>+</sup>, we used a modified aCSF of the following composition: 97 mM NaCl, 26 mM NaHCO<sub>3</sub>, 1.25 mM NaH<sub>2</sub>PO<sub>4</sub>, 30 mM KCl, 1 mM MgSO<sub>4</sub>, 1 mM CaCl<sub>2</sub>, and 10 mM D-glucose, equilibrated with 95%O<sub>2</sub>, 5% CO<sub>2</sub>. Patches were exposed to an isohydric hypercapnic solution with elevated K<sup>+</sup> concentrations: 43 mM NaCl, 80 mM NaHCO<sub>3</sub>, 1.25 mM NaH<sub>2</sub>PO<sub>4</sub>, 30 mM KCl, 1 mM MgSO<sub>4</sub>, 1 mM CaCl<sub>2</sub>, and 10 mM D-glucose, equilibrated with 12% CO<sub>2</sub>/88% O<sub>2</sub>.

#### Data analysis and statistics

To analyze how the single-channel current varied with transmembrane voltage and ionic conditions, a sum of Gaussian distributions was fitted (by a least-squares method) to an all-points histogram of channel activity at each transmembrane potential. The current amplitude of the unitary single-channel openings was estimated from these fits (mean of single-channel current minus mean of the noise). The single-channel conductance and reversal potentials were estimated by fitting lines to the linear portion of the current–voltage relation. Expected equilibrium potentials were calculated from the Nernst equation based on the composition of the solutions used in the patch pipette and bathing medium.

To analyze the effect of PCO<sub>2</sub> on channel gating, the open probability of the channel was estimated from all-points histograms. The area under the curve corresponding to single-channel or multiple-channel openings was obtained from a sum of up to four Gaussian distributions fitted to these histograms by a least-squares method. The area under the Gaussians that corresponded to 1, 2, or 3 simultaneous channel opening was expressed as a proportion of the total area under the entire curve. The veracity of the fitting procedure was additionally checked by comparing the total area from the all-points histogram (sum of the bins) and the area under the fitted Gaussians (from the integral); these values differed by no more than 2%.

To measure channel open times and fit exponential distributions, the data files were imported into WinEDR (written by John Dempster, University of Strathclyde) for analysis. Channel openings were detected via a threshold set at 50% of amplitude of the single-channel current. Careful selection of stretches of data ensured that there were very few multiple-channel openings included in the analysis. To facilitate parameter estimation, the data were then plotted as a histogram with logarithmically increasing bin widths with 16 bins per decade [26].

Unless otherwise noted, the values are given as mean ± SEM and *n* values refer to the number of patches.

## Results

### A small conductance channel is sensitive to alterations in CO<sub>2</sub>

In the course of studying the CO<sub>2</sub> sensitivity of connexins [11], we observed a small conductance channel in excised outside-out patches drawn from HeLa cells that exhibited sensitivity to changes in PCO<sub>2</sub>—the frequency of channel openings rapidly increased as the level of PCO<sub>2</sub> increased (Fig. 1a, b). As extracellular pH was kept constant while PCO<sub>2</sub> was changed (see “Methods”), the change in channel gating was unlikely to be due to alterations of extracellular pH. Equally changes in pH on the intracellular face of the membrane are also unlikely under this recording configuration as the excised patch has a very small membrane surface area, and it is improbable that CO<sub>2</sub> would be able to diffuse through the membrane patch at a sufficient rate to rapidly alter the pH of the patch recording solution and hence channel gating. The CO<sub>2</sub>-dependent opening of the channel is thus most likely due to the direct effects of CO<sub>2</sub> on the channel.

Increasing PCO<sub>2</sub> from its control value (35 mmHg) to 55 or 70 mmHg caused a progressively bigger increase in the frequency of channel openings such that multiple overlapping channel openings could readily be seen at these higher levels of PCO<sub>2</sub> (Fig. 1a–c). A reduction of PCO<sub>2</sub> to 20 mmHg resulted in a decrease in the frequency of channel openings (Fig. 1a–c).

To quantify these effects we estimated the open probability (*P*<sub>o</sub>) of the channel at different levels of PCO<sub>2</sub> (see “Methods”). Our analysis showed that *P*<sub>o</sub> increased with PCO<sub>2</sub> and could be fitted by the Hill equation assuming a Hill coefficient of 2 and a half-maximal activation of the channel at a PCO<sub>2</sub> of 45 mmHg (Fig. 1d).

### Channel open time distribution

We examined the distribution of channel open times at different levels of PCO<sub>2</sub>. Under control conditions (PCO<sub>2</sub> 35 mmHg), this distribution could be fitted by either one or the sum of two exponential distributions. This demonstrated a main open state with a mean open time of 2.1 ± 0.5 ms (*n* = 5). However in two of these cases, fitting a second distribution with a longer mean time constant gave a statistically significantly better fit (Fig. 2). We noticed that the prevalence of these longer time openings increased at higher levels of PCO<sub>2</sub>. In one case, it was possible to measure the mean open times at all four levels of PCO<sub>2</sub> (Fig. 2; Table 1). We found that while the short and long mean open times did not vary significantly at different levels of PCO<sub>2</sub>, the amplitude of the distribution with the longer mean open time scaled with PCO<sub>2</sub> (Table 1). This analysis

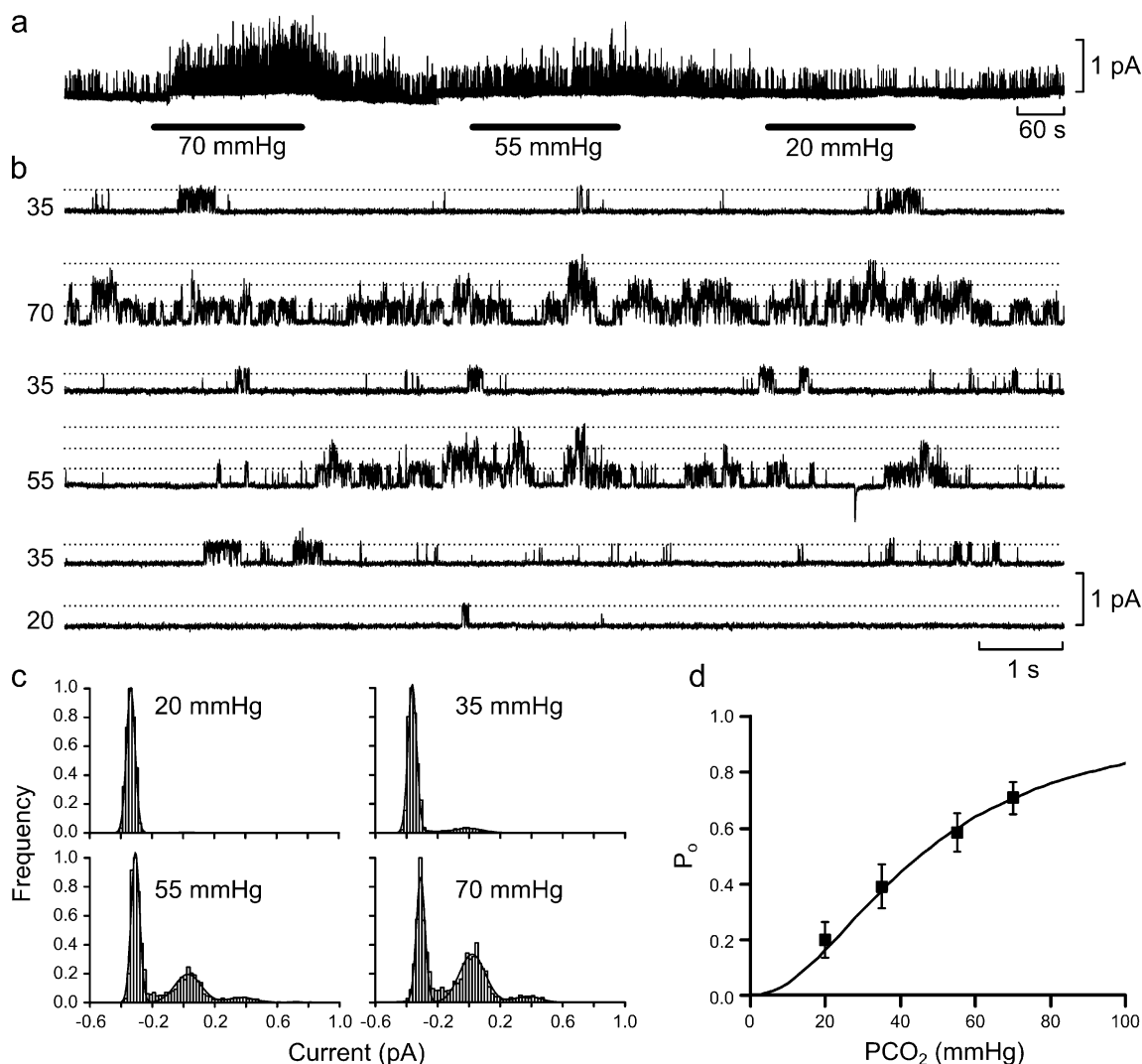


**Fig. 1** Increasing  $\text{PCO}_2$  increases open probability of a small conductance channel. **a** Continuous record of the effects of different  $\text{CO}_2$  concentrations on channel gating in outside-out patches from HeLa cells. Note that the effect of changing  $\text{PCO}_2$  from the control level of 35 mmHg to the levels marked on the *black bars* on channel gating was rapid. Isolated patch was held at +10 mV. **b** Expanded traces from **a** demonstrating the gating of the channels in the patch.

*Dotted lines* represent different levels of channel openings, and multiple openings are only seen at the higher levels of  $\text{PCO}_2$ . **c** All-points histograms obtained from the data in **b** and fitted with sums of Gaussian distributions to estimate  $P_o$ . **d** Plot of  $P_o$  vs  $\text{PCO}_2$  ( $n=5$  for each point; *bars* are SEMs). *Continuous line* is drawn to the Hill equation,  $P_o = 1/(1+(45/\text{PCO}_2)^2)$

suggests that increased levels of  $\text{CO}_2$  may increase  $P_o$  by promoting entry into a second open state that has a longer mean open time (measured over all levels of  $\text{PCO}_2$ ,  $7.0 \pm 1.0$  ms,  $n=3$ ).

The current–voltage relationship of the single-channel currents

We examined how the single-channel currents altered with voltage (Fig. 3a). The single-channel current exhibited inward rectification (Fig. 3b). The conductance of the channel was  $6.7 \pm 0.5$  pS (calculated from the linear portion of the  $I$ – $V$  relation,  $n=4$ , Fig. 3b) and the single-channel

currents reversed at  $-70$  mV (Fig. 3a, b). This reversal potential lay between the  $\text{K}^+$  and  $\text{Cl}^-$  equilibrium potentials calculated to be  $-93$  mV and  $-20$  mV, respectively. Interestingly  $P_o$  showed little variation at different potentials (Fig. 3c).

We tested the nature of the permeant ion by altering extracellular  $\text{K}^+$  concentration. A tenfold increase in  $\text{K}^+$  concentrations moved the reversal potential to  $-9$  mV (Fig. 3a, b). This shift in reversal potential was similar to that predicted by the Nernst equation, suggesting that this channel has high selectivity for  $\text{K}^+$ . Interestingly, in the presence of elevated extracellular  $\text{K}^+$ , the single-channel conductance increased to  $11.5 \pm 0.5$  pS (calculated from the

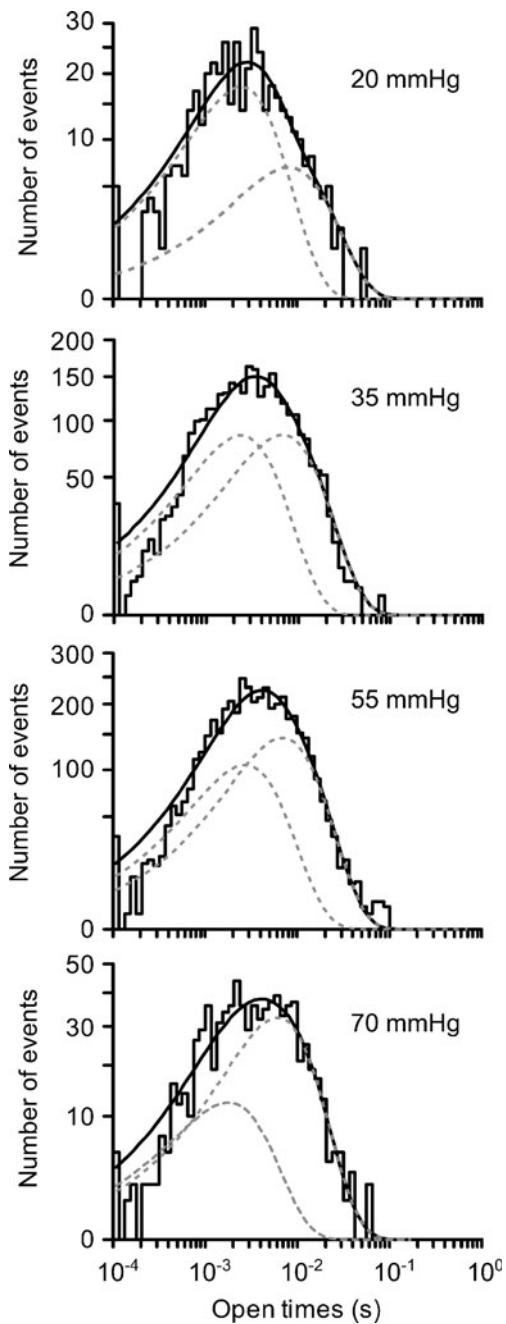


**Fig. 2** Channel open time distributions recorded at different levels of  $\text{PCO}_2$ . Analysis of raw data from Fig. 1. The solid line is the combined fit of two exponential distributions, each shown separately as grey dashed lines. At each level of  $\text{PCO}_2$ , the fitting of two exponential distributions gave a statistically significantly better fit than a single exponential ( $P < 0.02$ ,  $F$  test). The effects of 55 and 70 mmHg on channel open times are probably underestimated as these were taken from stretches of data early in the application of the elevated  $\text{PCO}_2$  to minimize the occurrence of multiple-channel openings

linear portion of the  $I$ - $V$  relation,  $n=4$ , Fig. 3b). The dependence of the single-channel conductance on extracellular  $[\text{K}^+]$  is characteristic of Kir channels.

A tenfold reduction of external chloride had no effect on the reversal potential ( $-70$  mV,  $n=3$ ), the single-channel

**Table 1** Dependence of mean open time on  $\text{PCO}_2$ . Fitting parameters from analysis in Fig. 2. At all levels of  $\text{PCO}_2$  channel open time distributions were best fitted by a sum of two exponential distributions:  $A_1 \exp(-t/\tau_1) + A_2 \exp(-t/\tau_2)$ . The amplitude of the distribution with the longer mean open time ( $A_2$ ) increased with  $\text{PCO}_2$ , suggesting that entry into this state was enhanced by  $\text{CO}_2$ . All numbers are given as mean  $\pm$  standard deviation (this latter value being associated with the accuracy of the fitting procedure)

$\text{PCO}_2$ (mmHg)	$\tau_1$ (ms)	$\tau_2$ (ms)	$A_2$ (%)
20	$2.4 \pm 0.5$	$8.0 \pm 4.1$	$30 \pm 20$
35	$2.4 \pm 0.5$	$6.8 \pm 1.3$	$53 \pm 16$
55	$2.7 \pm 0.7$	$6.9 \pm 1.2$	$61 \pm 20$
70	$1.8 \pm 0.7$	$6.1 \pm 0.9$	$77 \pm 16$

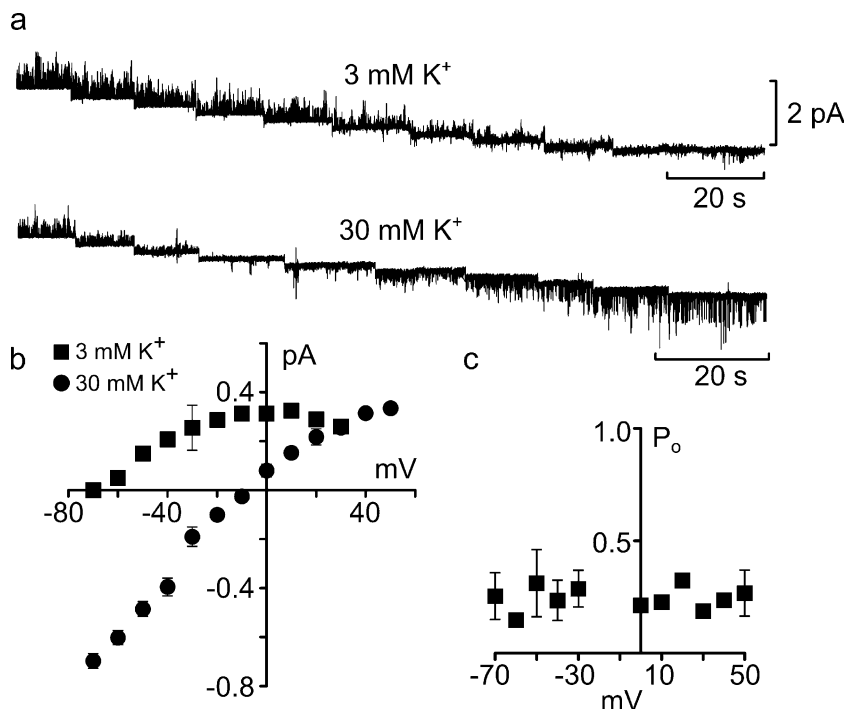
inward rectification or conductance (Fig. 4a). However, we found that this reduction of the concentration of extracellular  $\text{Cl}^-$  often lowered the holding current and reduced basal noise levels (Fig. 4b). Thus, there appeared to be a persistent  $\text{Cl}^-$  current carried by a channel closely located to the  $\text{K}^+$  channel, which can obscure the gating of the  $\text{K}^+$  channel.

## Discussion

Channels of the Kir family exhibit varying degrees of inward rectification show a single-channel conductance that varies with extracellular  $\text{K}^+$  concentration and are not blocked by TEA [9]. As these are all features of the channel that we have described, the  $\text{CO}_2$ -sensitive channel is most probably an exemplar of the Kir family some of which, for example Kir1.1, exhibit only relatively weak inward rectification [29].

The sensitivity of  $\text{K}^+$  channels to fluctuations in pH is widespread and has received much attention with respect to possible physiological functions in chemosensing [6, 16, 17, 30]. Several members of the Kir family are sensitive to pH and acidification causes these channels to close hence giving depolarization. Some of these channels, especially Kir4.1 and 5.1, are favored candidates to participate in chemosensing [13, 31, 32]. However, other Kir channels (notably Kir1.1) are also present in both the carotid body and in areas of the medulla oblongata that participate in chemosensing [25, 31]. Interestingly, the Kir channel that we have described opens with increases in  $\text{PCO}_2$ . Increasing levels of  $\text{PCO}_2$  under physiological conditions would normally cause both extracellular and intracellular acidification. The net effect of a combined change in pH and  $\text{PCO}_2$  (the more usual physiological circumstance) on this variant of the Kir family would therefore depend upon its relative sensitivity to changes in pH versus changes in  $\text{PCO}_2$ . Different members of the Kir family are distinguishable on

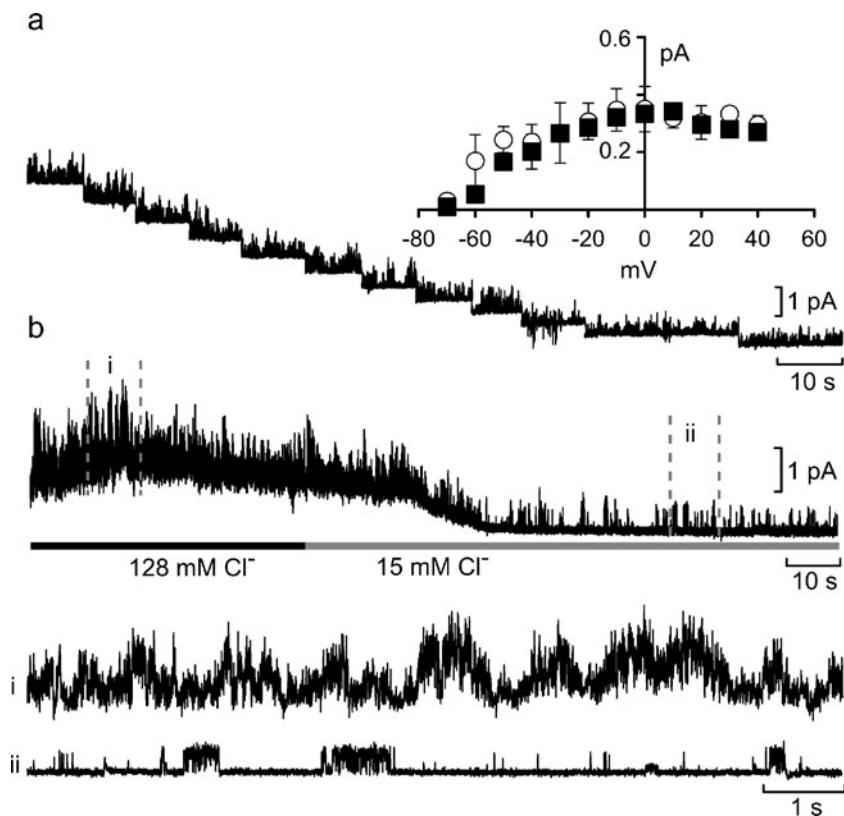
**Fig. 3** Current–voltage characteristics and permeability of the CO<sub>2</sub>-sensitive channel. **a** Single-channel gating in outside-out excised patches during a series of 10 mV steps from +20 mV to –70 mV (left to right) in control 3 and 30 mM K<sup>+</sup> aCSF at a PCO<sub>2</sub> of 70 mmHg. **b** Current–voltage plots of the single-channel currents in 3 mM K<sup>+</sup> (n=4) and 30 mM K<sup>+</sup> (n=4) aCSF. The reversal potential changed from –70 mV to –9 mV and the slope conductance of the channel was increased by elevating extracellular K<sup>+</sup>. **c** Plot of the open probability (P<sub>o</sub>) against membrane potential for three excised patches, measured in 30 mM K<sup>+</sup> aCSF. P<sub>o</sub> exhibited no voltage dependence. Bars are SEMs



the basis of their pH sensitivity, for example Kir1.1 is insensitive to *extracellular* pH and requires *intracellular* acidification for closure [33]. However, it remains unknown whether an increase in PCO<sub>2</sub> at constant intracellular pH will enhance current through Kir1.1 [33]. A common consensus

is that alterations in PCO<sub>2</sub> levels are sensed through consequent changes in either extracellular or intracellular pH. This is partly because until now there have been few mechanisms proposed by which CO<sub>2</sub> could be detected directly. However, we have recently shown that CO<sub>2</sub> can

**Fig. 4** Colocalization of Cl<sup>-</sup> and K<sup>+</sup> channels in excised patches. **a** Current–voltage relationship of single-channel currents recorded in an outside-out patch in the presence of 15 mM Cl<sup>-</sup> in the medium at a PCO<sub>2</sub> of 70 mmHg. The holding potential was changed from +40 to –70 mV in 10-mV steps (left to right). The inset shows the summary graph comparing the I–V relations for control (n=7, black squares) and lowered Cl<sup>-</sup> aCSF (n=3, open circles). Bars are SEMs. **b** A continuous current record from the patch before and during the application of low Cl<sup>-</sup> aCSF. Portions of the record in control aCSF (i) and low Cl<sup>-</sup> aCSF (ii) are shown below. Note that the reduction of extracellular Cl<sup>-</sup> ions reduces both the holding current and basal noise. Outside-out patch held at +10 mV



interact directly with connexins [11, 12] causing them to open and release ATP. Our present results suggest that at least one member of the Kir family also exhibits direct sensitivity to CO<sub>2</sub>. Interestingly although Kir channels are tetrameric, the relationship of  $P_o$  versus PCO<sub>2</sub> can be fitted with a Hill coefficient of 2 possibly indicating that only two molecules of CO<sub>2</sub> need to bind to the channel to enhance opening. Our finding that elevated levels of PCO<sub>2</sub> increase the occurrence of a second open state with a longer mean open time could imply that binding of CO<sub>2</sub> to the channel promotes entry into this second open state.

How the K<sup>+</sup> channel reported here might fit into a physiological system would depend on where it is expressed. In non-excitabile cells of secretory tissues, opening of K<sup>+</sup> channels and consequent K<sup>+</sup> efflux causes secretion in exocrine glands; thus most secretions have elevated K<sup>+</sup>. CO<sub>2</sub>-dependent secretion involving a K<sup>+</sup> channel has been found in tissue slices of the parotid gland, though this appears to be due to the stimulation of a second messenger [28] such as soluble adenylyl cyclase [3, 35]. In pancreatic acinar cells, a low conductance (17 pS at symmetrical K<sup>+</sup> concentrations) inwardly rectifying TEA-insensitive channel has been described [23, 24].

We commonly found that a Cl<sup>-</sup> current was also present in the excised patches along with the K<sup>+</sup> channel. There is a precedent for Kir channels, notably Kir1.1, being localized with the CFTR Cl<sup>-</sup> channel in the apical membrane of cells in the thick ascending limb of the loop of Henlé in the kidney [9]. In many secretory systems, Cl<sup>-</sup> and K<sup>+</sup> channels colocalize to ensure that K<sup>+</sup> efflux from the cell is accompanied by chloride extrusion into the extracellular space [27]. Secretory cells such as parotid acinar cells express several chloride ion channels, which control extrusion and re-uptake of chloride ions from the cell [15].

Kir channels in the central nervous system help to control the resting potential. In all cases, so far reported Kir channels close in response to acidification, thus giving pH-dependent depolarization. The surprising implication of our results is that increasing CO<sub>2</sub> would cause the opening of this particular Kir channel and hence lead to hyperpolarization. This could therefore be a mechanism that contributes to inhibitory processes occurring during hypercapnia. Such processes have been described. For example, slowly adapting pulmonary stretch receptors (SARs) are inhibited during hypercapnia by the activation of a TEA-insensitive potassium channel [14]. This inhibition has been previously attributed to alterations in extracellular pH as acetazolamide, a carbonic anhydrase inhibitor, significantly altered the response of SARs to CO<sub>2</sub> [14]. Interestingly Kir channels, including Kir1.1, have been described in the NTS, an area where the SARs terminate onto their second-order cells [32]. Alternatively, this channel may play a role in the hyperpolarization of GABAergic and glycinergic neurons, which

would lead to disinhibition of neural networks. Disinhibition occurs frequently in the cardiorespiratory network during hypercapnia [10]; it leads to a loss of glycinergic inputs in the cardioinhibitory vagal neurons and inspiratory-related GABAergic inputs [10]. These GABAergic inputs may come from the raphé magnus [1]. Were this channel expressed on these neurons, an increase in CO<sub>2</sub> would inhibit them and remove the GABAergic input into the pre-Böttinger, leading to an increase in respiration.

**Acknowledgments** We thank the Medical Research Council and Biotechnology and Biological Sciences Research Council for support.

**Open Access** This article is distributed under the terms of the Creative Commons Attribution Noncommercial License which permits any noncommercial use, distribution, and reproduction in any medium, provided the original author(s) and source are credited.

## References

1. Cao Y, Fujito Y, Matsuyama K, Aoki M (2006) Effects of electrical stimulation of the medullary raphé nuclei on respiratory movement in rats. *J Comp Physiol* 192:497–505
2. Catron TF, Powell FL, West JB (2006) A strategy for determining arterial blood gases on the summit of Mt. Everest. *BioMed Central Physiol* 6:1–6
3. Chen Y, Cann MJ, Litvin TN, Lourgenko V, Sinclair ML, Levin LR, Buck J (2000) Soluble adenylyl cyclase as an evolutionary conserved bicarbonate sensor. *Science* 289:625–627
4. Feldman JL, Mitchell GS, Nattie EE (2003) Breathing: rhythmicity, plasticity, chemosensitivity. *Annu Rev Neurosci* 26:239–266
5. Filosa JA, Putnam RW (2003) Multiple targets of chemosensitive signaling in locus coeruleus neurons: role of K<sup>+</sup> and Ca<sup>2+</sup> channels. *Am J Physiol Cell Physiol* 53:C145–C155
6. Guyenet PG (2008) The 2008 Carl Ludwig lecture: retrotrapezoid nucleus, CO<sub>2</sub> homeostasis, and breathing automaticity. *J Appl Physiol* 105:404–416
7. Guyenet PG, Stornetta RL, Bayliss DA, Mulkey DK (2005) Retrotrapezoid nucleus: a litmus test for the identification of central chemoreceptors. *Exp Physiol* 90:247–257
8. Haldane JS, Priestley JG (1905) The regulation of lung ventilation. *J Physiol* 32:225–266
9. Hibino H, Inanobe A, Furutani K, Murakami S, Findlay I, Kurachi Y (2010) Inwardly rectifying potassium channels: their structure, function, and physiological roles. *Physiol Rev* 90:291–366
10. Huang Z-G, Griffioen KJS, Wang X, Dergacheva O, Kamendi H, Gorini C, Bouairi E, Mendelowitz D (2006) Differential control of central cardiorespiratory interactions by hypercapnia and the effect of prenatal nicotine. *J Neurosci* 26:21–29
11. Huckstepp RTR, Eason R, Sachdev A, Dale N (2010) CO<sub>2</sub>-dependent opening of connexin 26 and related  $\beta$  connexins. *J Physiol* 588:3921–3931
12. Huckstepp RTR, Id Bihi R, Eason R, Spyer KM, Dicke N, Willecke K, Marina N, Gourine AV, Dale N (2010) Connexin hemichannel-mediated CO<sub>2</sub>-dependent release of ATP in the medulla oblongata contributes to central respiratory chemosensitivity. *J Physiol* 588:3901–3920
13. Jiang C, Xu H, Cui N, Wu J (2001) An alternative approach to the identification of respiratory central chemoreceptors in the brainstem. *Respir Physiol* 129:141–157



14. Matsumoto S, Takahashi T, Tanimoto T, Saiki C, Takeda M (1999) Effects of potassium channel blockers on CO<sub>2</sub>-induced slowly adapting pulmonary stretch receptor inhibition. *J Pharmacol Exp Therap* 290:974–979
15. Melvin JE (1999) Chloride channels and salivary gland function. *Crit Rev Oral Biol Med* 10:199–209
16. Mulkey DK, Stornetta RL, Weston MC, Simmons JR, Parker A, Bayliss DA, Guyenet PG (2004) Respiratory control by ventral surface chemoreceptor neurons in rats. *Nat Neurosci* 7:1360–1369
17. Mulkey DK, Talley EM, Stornetta RL, Siegel AR, West GH, Chen X, Sen N, Mistry AM, Guyenet PG, Bayliss DA (2007) TASK channels determine pH sensitivity in select respiratory neurons but do not contribute to central respiratory chemosensitivity. *J Neurosci* 27:14049–14058
18. Peers C, Buckler KJ (1995) Transduction of chemostimuli by the type 1 carotid body cell. *J Membr Biol* 144:1–9
19. Pineda J, Aghajanian GK (1997) Carbon dioxide regulates the tonic activity of locus coeruleus neurons by modulating a proton- and polyamine-sensitive inward rectifier potassium current. *Neuroscience* 77:723–743
20. Putnam RW, Filosa JA, Ritucci NA (2004) Cellular mechanisms involved in CO<sub>2</sub> and acid signalling in chemosensitive neurons. *Am J Physiol Cell Physiol* 287:C1493–C1526
21. Richerson GB (2004) Serotonergic neurons as carbon dioxide sensors that maintain pH homeostasis. *Nat Rev Neurosci* 5:449–461
22. Ritucci NA, Erlichman JS, Leiter JC, Putnam RW (2005) Response of membrane potential and intracellular pH to hypercapnia in neurons and astrocytes from rat retrotrapezoid nucleus. *Am J Physiol—Regulat Integr Compar Physiol* 289:851–861
23. Schmid A, Feick P, Schulz I (1997) Inwardly rectifying, voltage-dependent and resting potassium currents in rat pancreatic acinar cells in primary culture. *J Physiol* 504:259–270
24. Schmid A, Schulz I (1995) Characterization of single potassium channels in mouse pancreatic acinar cells. *J Physiol* 484:661–676
25. Schultz J-H, Czachurski J, Volk T, Ehmke H, Seller H (2003) Central sympathetic chemosensitivity and Kir1 potassium channels in the cat. *Brain Res* 963:113–120
26. Sigworth FJ, Sine SM (1987) Data transformations for improved display and fitting of single-channel dwell time histograms. *Biophys J* 52:1047–1054
27. Sørensen JB, Nielsen MS, Gudme CN, Larsen EH, Nielsen R (2001) Maxi K<sup>+</sup> channels co-localised with CFTR in the apical membrane of an exocrine gland acinus: possible involvement in secretion. *Pflügers Arch—Euro. J Physiol* 442:1–11
28. Takahata T, Hayashi M, Ishikawa T (2003) SK4/IK1-like channels mediate TEA-insensitive, Ca<sup>2+</sup>-activated K<sup>+</sup> currents in bovine parotid acinar cells. *Am J Physiol Cell Physiol* 284:C127–C144
29. Wang W-H (2006) Regulation of ROMK (Kir1.1) channels: new mechanisms and aspects. *Am J Physiol Renal Physiol* 290:F14–F19
30. Wellner-Kienitz M-C, Shams H, Scheid P (1998) Contribution of Ca<sup>2+</sup>-activated K<sup>+</sup> channels to central chemosensitivity in cultivated neurons of fetal rat medulla. *J Neurophysiol* 79:2885–2894
31. Wu J, Xu H, Shen W, Jiang C (2004) Expression and coexpression of CO<sub>2</sub>-sensitive Kir channels in brainstem neurons of rats. *J Membr Biol* 197:179–191
32. Yamamoto Y, Ishikawa R, Omoe K, Taniguchi K (2008) Expression of inwardly rectifying K<sup>+</sup> channels in the carotid body of rat. *Histol Histopathol* 23:799–806
33. Zhu G, Liu C, Qu Z, Chanchevalap S, Xu H, Jiang C (2000) CO<sub>2</sub> inhibits specific inward rectifier K<sup>+</sup> channels by decreases in intra- and extracellular pH. *J Cell Physiol* 183:53–64
34. Ziemann AE, Allen JE, Dahdaleh NS, Drebot II, Coryell MW, Wunsch AM, Lynch CM, Faraci FM, Howard MA, Welsh MJ, Wemmie JA (2009) The amygdala is a chemosensor that detects carbon dioxide and acidosis to elicit fear behavior. *Cell* 139:1012–1021
35. Zippin JH, Levin LR, Buck J (2001) CO<sub>2</sub>/HCO<sub>3</sub><sup>-</sup>-responsive soluble adenylyl cyclase as a putative metabolic sensor. *Trends Endocrinol Metab* 12:366–370